

Cubic InN growth on sapphire (0001) using cubic indium oxide as buffer layer

J. G. Lozano,^{a)} F. M. Morales, R. García, and D. González

Departamento de Ciencia de los Materiales e Ingeniería Metalúrgica y Química Inorgánica, Facultad de Ciencias, Universidad de Cádiz, Puerto Real, Cádiz 11510, Spain

V. Lebedev, Ch. Y. Wang, V. Cimalla, and O. Ambacher

Institute of Micro- and Nanotechnologies, Technical University Ilmenau, D-98684 Ilmenau, Germany

(Received 14 December 2006; accepted 19 January 2007; published online 26 February 2007)

Cubic InN layers were grown by molecular beam epitaxy on buffer layers of indium oxide prepared onto sapphire (0001) substrates. The structure was analyzed by means of electron diffraction and transmission electron microscopy. The intermediate indium oxide layer presents a body centered cubic (bcc) structure, with $\text{bcc-In}_2\text{O}_3(001)\parallel\text{Al}_2\text{O}_3(0001)$ plane relationship. Thereupon, a zinc-blende phase of InN (001) was grown with a reticular misfit of 1.6% and a significant reduction of mismatch-related defects. This good coherence offers a promising expectation to obtain high quality cubic InN layers superior to other highly mismatched cubic substrates used previously.

© 2007 American Institute of Physics. [DOI: 10.1063/1.2696282]

Indium nitride has recently attracted much attention due to its enormous potential as a consequence of its outstanding properties such as the smallest effective electron mass, largest mobility, highest saturation velocity, and smallest direct band gap among the nitride semiconductors.¹ Up to now, the huge majority of research on InN has been concentrated on the hexagonal wurtzite (2H polytype) form (*h*-InN), which is the thermodynamic stable phase at usual growth conditions. Nevertheless, cubic InN (*c*-InN) with zinc-blende structure is also interesting because it is predicted to possess superior electronic properties for device applications.² For instance, since the lattice of zinc-blende structure is isotropic, phonon scattering would be lowered, and it is expected to achieve a higher saturated electron drift velocity than in the wurtzite structure.³ Besides this, a special attention on its optical properties exists. The direct band gap of wurtzite InN films is accepted to be 0.65–0.69 eV.^{4,5} For cubic InN, the band gap could not be determined yet since up to date no thick layers of *c*-InN were available. In all the cases, the band gap energy of *c*-InN is expected to be slightly below the one of *h*-InN. Recent calculations propose a band gap of 0.53 eV,⁶ which would expand the applications of group-III nitrides more towards the infrared region.

However, the improvement of the structural quality of *c*-InN layers is still a challenge, which is difficult to solve due to the lack of suitable substrates. Up to date, publications about *c*-InN have appeared very scarcely. In the past decade, structural properties of *c*-InN films grown on GaAs(001),⁷ GaAs(111),⁸ and (001) yttria-stabilized cubic zirconia⁹ substrates were reported. The best attempt to grow cubic phase has been using an InAs interlayer on GaAs(001), although the *c*-InN contained a very high density of stacking faults due to the large mismatch with the InAs intermediate layer.¹⁰ In all these cases, zinc-blende InN was grown on a substrate with a zinc-blende crystal structure. However, sapphire is the most extensively used substrate material for the epitaxial growth of III-N compounds. Large area, good quality crys-

tals of sapphire are easily available at relatively low cost, being transparent and stable at high temperature. To date, the best quality epitaxial films of *h*-InN have been grown on sapphire substrates by means of the incorporation of buffer layers such as AlN and GaN, which improve greatly the structural and electrical properties of InN films.¹¹ *c*-InN on sapphire was only obtained at low temperatures either as isolated domains inside *h*-InN layers on *c*-plane sapphire¹¹ or as film on *r*-plane sapphire.¹²

On the other hand, doped indium oxide has become of special interest for semiconductor device manufacturers as a material for *p*-Ohmic contacts in III-N devices.¹³ The need to improve the contact resistance and the light transmission efficiency for nitride light-emitting diodes (LEDs) could be fulfilled by the use of (Cu, Sn, Ga, or Zn) doped indium oxide that shows a high transparency in the visible spectral region, a high electrical conductivity, and a high work function.¹³ The integration of a high efficiency transparent conductive oxide such as In_2O_3 with a promising active layer such as InN becomes a good approach for yielding high performance metal-semiconductor-metal photodiodes or photo-switching devices.

In this letter, we show the potential of indium oxide as a buffer layer for the growth of InN onto sapphire (0001) substrates. The occurrence of the cubic phase of InN and its epitaxial matching with indium oxide are demonstrated. The heterostructure formed by *c*-InN and In_2O_3 could become an established couple for the development of InN-based LEDs or metal-oxide-semiconductor field-effect transistors.

All InN samples referred in this work were grown by plasma induced molecular beam epitaxy (PIMBE) on *ex situ* prepared indium oxide epitaxial templates. 520 nm thick $\text{bcc-In}_2\text{O}_3(001)$ films used as buffer layers were grown in a horizontal metal organic chemical vapor deposition (MOCVD) reactor on (0001) sapphire substrates. The detailed description of the growth conditions for PIMBE of InN (Ref. 10) and MOCVD of $\text{bcc-In}_2\text{O}_3$ (Ref. 14) has been reported elsewhere. Structural analysis was also performed by high resolution x-ray diffraction (HR-XRD) using a Bruker D8 diffractometer. Selected area electron diffraction (SAED)

^{a)} Author to whom correspondence should be addressed; FAX: +34 956 01 62 88; electronic mail: juangabriel.lozano@uca.es

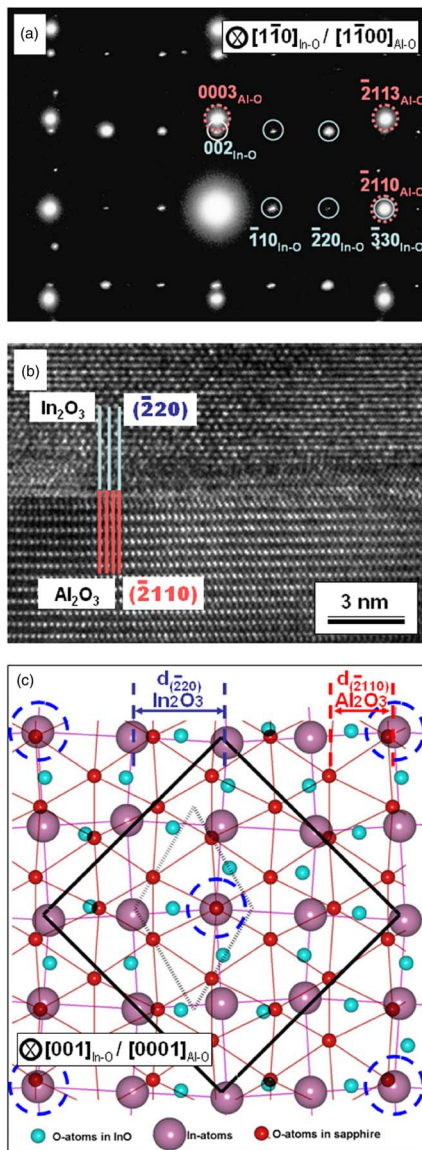


FIG. 1. (a) XTEM SAED pattern along the $[1\bar{1}0]$ zone axis of In_2O_3 (blue circles) and $[1\bar{1}00]$ of sapphire (red circles). (b) HRTEM image taken along the same direction. (c) Schematic diagram showing the superposition just at the interface between the O atoms of $\text{Al}_2\text{O}_3(0001)$ (red atoms) and $\text{In}_2\text{O}_3(001)$ where the O sublattice (light blue atoms) and the In sublattice (cyan atoms) are displayed. Solid and dashed lines draw the projection of the unit cells of bcc- In_2O_3 and sapphire, respectively. The fitting of three $(\bar{2}\bar{2}0)$ In_2O_3 planes with four $(\bar{2}\bar{1}10)$ sapphire planes is visible.

and high resolution transmission electron microscopy (HRTEM) in cross section TEM (XTEM) specimens were carried out in a JEOL 2011 and a JEOL 2010 field emission gun, both working at 200 kV.

Figure 1 displays a HRTEM micrograph and a SAED pattern of the interface between sapphire and the In_2O_3 layer. The analysis of the diffraction patterns [Fig. 1(a)] shows that In_2O_3 crystallizes in a body centered cubic structure with an in-plane epitaxial relationship of $\text{In}_2\text{O}_3(001)\parallel\alpha\text{-Al}_2\text{O}_3(0001)$. This cubic phase of In_2O_3 consists of the so-called bixbyite structure with the $Ia\bar{3}$ space group, having a complex unit cell which contains 80 atoms. The lattice parameter was estimated from HRTEM images using the relaxed sapphire as reference. The measured value of 10.1(3) Å is in a good agreement with previously reported

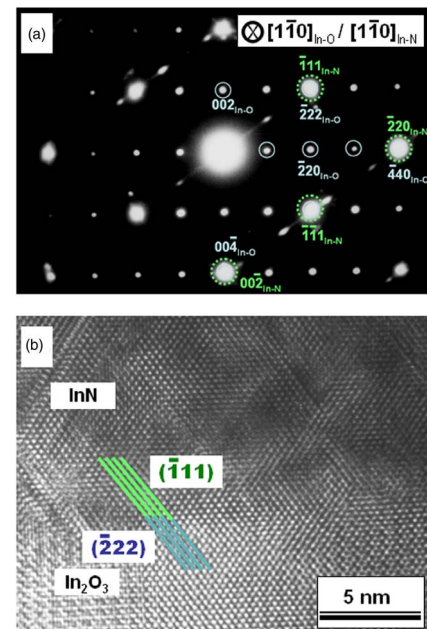


FIG. 2. (a) Cross section SAED pattern along the $[1\bar{1}0]$ pole of the interface between bcc- In_2O_3 (light blue circles) and $c\text{-InN}$ (light red circles). (b) HRTEM image of the interface along the same pole. Inside, intercepting fringes indicate the good coherence between the $\{111\}$ planes of both layers.

lattice parameter of 10.1192 Å.¹⁵ The epitaxial relationship has been verified [see Fig. 1(b)] as $\text{In}_2\text{O}_3[001]\parallel\text{Al}_2\text{O}_3[0001]$ and $\text{In}_2\text{O}_3[1\bar{1}0]\parallel\text{Al}_2\text{O}_3[1\bar{1}00]$. The lattice mismatch between Al_2O_3 and bcc- In_2O_3 is better described by comparing the average spacing between oxygen atoms in the $(\bar{2}\bar{1}10)$ sapphire planes, 2.382 Å, with the average spacing of In atoms at the $(\bar{2}\bar{2}0)$ bcc- In_2O_3 planes, 3.577 Å. From this result, a lattice mismatch of 50.0% is calculated. Figure 1 shows the scheme of the superposition of both interfaces. There, the Al_2O_3 unit cell is symbolized by a dashed line (rhombus) and only those O atoms from sapphire placed just at the interface plane are displayed. The unit cell of In_2O_3 is also represented by a solid line (square) and both In and O near-interface sublattices are displayed. The almost total coincidence between In and O (from sapphire) atoms is marked by blue circles. As we can see in the figure, an approximate matching of three $(\bar{2}\bar{2}0)$ bcc- In_2O_3 planes of the film with four $(\bar{2}\bar{1}10)$ planes of the sapphire is in good agreement with the HRTEM images [Fig. 1(b)]. These extra half planes define an orthogonal dislocation network which is formed in a high percentage from the beginning of the film growth. A geometrical misfit dislocation network with a linear density of $1.3\times 10^7\text{ cm}^{-1}$, arising from a different mechanism in comparison with the classical van der Merwe–Matthews type,¹⁶ accommodates most of the mismatch from the first monolayers. We also highlight that, in spite of the very high density of misfit dislocations, the formation of threading dislocations driven through the indium oxide is very low.

InN layers were grown over the In_2O_3 -bcc structures, and Fig. 2(a) shows a SAED pattern of both layers. The indexing of the diffraction pattern proved that InN grows in a zinc-blende structure where (001) $c\text{-InN}$ planes are parallel to bcc- $\text{In}_2\text{O}_3(001)$ planes. This epitaxial relationship can also be verified from HRTEM images of the interface [Fig. 2(b)] as bcc- $\text{In}_2\text{O}_3[001]\parallel c\text{-InN}[001]$ and bcc-

$\text{In}_2\text{O}_3[1\bar{1}0]\parallel c\text{-InN}[1\bar{1}0]$. The lattice parameter of $c\text{-InN}$ was estimated to be 4.9(8) Å, which is in a good agreement with previously reported values for epilayers grown on $\text{InAs}(001)$ (Ref. 10) (5.04 Å), on $\text{GaAs}(001)$ (Ref. 7) (4.98 Å), and on $r\text{-plane sapphire}$ ¹² (4.986 Å) substrates. Using the SAED pattern it is possible to appreciate the spatial coincidence between the $\{111\}$ diffraction vectors of the $c\text{-InN}$ with the $\{222\}$ diffraction vectors of the $\text{bcc-In}_2\text{O}_3$. This match is easy to verify from the HRTEM images of this interface [see Fig. 2(b)], where an excellent correspondence is observed implying a very low density of misfit dislocations lying at the interface.

The polytype of the InN layers was confirmed by $\theta/2\theta$ HR-XRD experiments. In agreement with the TEM results, there are no hexagonal peaks related to the presence of $w\text{-InN}$ phase. However, $c\text{-InN}$ peak is weaker and worse than InO one. Up to now, $\text{bcc-In}_2\text{O}_3$ surface is greatly textured,¹⁴ which likely limits the growth of large InN domains. It means that quality of $c\text{-InN}$ for fabrication of high performance devices is a challenge that powerfully depends on the improvement of the $\text{bcc-In}_2\text{O}_3(001)$ growth.

We have demonstrated the possibility to obtain zinc-blende InN layers on sapphire using $\text{bcc-In}_2\text{O}_3(001)$ as buffer layer. However, wurtzite is the most common crystal structure of group-III nitrides (except for BN). InN is not an exception and we may analyze why the less thermodynamically favored phase is promoted in this case. In the framework of the density functional theory, Mancera *et al.*¹⁷ predict that the total energy of cubic InN is only 40 meV/unit higher than for hexagonal InN. Zoroddu *et al.*¹⁸ proposed that this difference is even lower (17 meV). This small difference in total energy explains why the two structures can be obtained experimentally depending on the substrate and the growth conditions. For comparison, the predicted difference per unit is 16 meV for GaN which implies that InN can be grown as easy as GaN in the cubic polytype.¹⁸

In our case, we propose that two factors lead to a preferential nucleation of the cubic polytype surpassing the small energetic barrier of the phase transition. Firstly, the fourfold symmetry of the (001) $\text{bcc-In}_2\text{O}_3$ surface constitutes the main driving force to replicate the squared atomic configuration characteristic of the zinc-blende phase. Secondly, the excellent match between these planes and the (001) $c\text{-InN}$ planes leads to a very low stress in the interface region. Highly stressed sites can work as activity centers to promote the wurtzite phase transformation since the estimated fault energies in the zinc-blende InN are all negative.¹⁹ Indeed, some $c\text{-InN}$ regions with a high density of stacking faults were observed demonstrating the metastability of the cubic phase even in such a low mismatched system, being an additional consideration to be taken into account in order to control carefully the growth conditions. The use of lower growth temperatures and an enhancement of the quality of the interface (flatter In_2O_3 surfaces) may reduce local stress concentrations and could be the key to limit the stacking fault formation.

Besides this, the improvement of the crystalline quality of the In_2O_3 buffer layer is a current challenge because the highly textured surface of the $\text{bcc-In}_2\text{O}_3(001)$ (Ref. 14) is a handicap to overcome for the development of functional de-

vices. As an example, InN growth on another crystallographic plane, as, for instance, the $\text{bcc-In}_2\text{O}_3(111)$, would reduce the lattice mismatch up to 30% and could suppress the disorientation observed among $\text{bcc-In}_2\text{O}_3$ domains inside the epitaxial layer. However, the advantage of growing InN on a fourfold symmetry template would be lost. The growth of In_2O_3 layers on sapphire is recent, and further studies are needed for understanding its nature and improving the film quality.

In summary, it was demonstrated that a buffer layer of In_2O_3 on (0001) sapphire substrates can be used for the growth of zinc-blende InN layers. Indium oxide buffer layers presented a bcc structure with $\text{In}_2\text{O}_3(001)\parallel\text{Al}_2\text{O}_3(0001)$ plane relationship. Zinc-blende InN(001) was deposited onto the buffer layer showing a low reticular mismatch of 1.6% and a low density of threading dislocations. The good assembly between $c\text{-InN}(001)$ and $\text{bcc-In}_2\text{O}_3(001)$ makes them an excellent candidate to integrate high quality $c\text{-InN}$ layers with high electrical conductivity $p\text{-Ohmic}$ contacts for III-N devices.

This work was supported by the CICYT Project No. MAT2004-01234 (Spain), by the Project No. TEP383 (Junta de Andalucía), and by Thüringer MWTA under Grant No. 2011420176 (INOZON).

¹S. O'Leary, B. Foutz, M. Shur, and L. Eastman, Appl. Phys. Lett. **88**, 152113 (2006).

²D. Bagayoko, L. Franklin, and G. L. Zhao, J. Appl. Phys. **96**, 4297 (2004).

³D. N. Talwar, D. Sofranko, C. Mooney, and S. Tallo, Mater. Sci. Eng., B **90**, 269 (2002).

⁴G. Koblmüller, C. S. Gallinat, S. Bernardis, J. S. Speck, G. D. Chern, E. D. Readinger, H. Shen, and M. Wraback, Appl. Phys. Lett. **89**, 071902 (2006).

⁵R. Goldhahn, A. T. Winzer, V. Cimalla, O. Ambacher, C. Cobet, W. Richter, N. Esser, J. Furthmüller, F. Bechstedt, H. Lu, and W. J. Schaff, Superlattices Microstruct. **36**, 591 (2004).

⁶P. Rinke, M. Scheffler, A. Qteish, M. Winkelnkemper, D. Bimberg, and J. Neugebauer, Appl. Phys. Lett. **89**, 161919 (2006).

⁷D. Chandrasekhar, D. J. Smith, S. Strite, M. E. Lin, and H. Morkoc, J. Cryst. Growth **152**, 135 (1995).

⁸A. Yamamoto, Y. Yamauchi, M. Ohkubo, and A. Hashimoto, J. Cryst. Growth **174**, 641 (1997).

⁹P. A. Anderson, C. E. Kendrick, T. E. Lee, W. Diehl, R. J. Reeves, V. J. Kennedy, A. Markwitz, R. J. Kinsey, and S. M. Durbin, Mater. Res. Soc. Symp. Proc. **798**, Y12.3 (2003).

¹⁰A. P. Lima, A. Tabata, J. R. Leite, S. Kaiser, D. Schikora, B. Schöttker, T. Frey, D. J. As, and K. Lischka, J. Cryst. Growth **201/202**, 396 (1999).

¹¹V. Lebedev, V. Cimalla, J. Pezoldt, M. Himmerlich, S. Krischok, J. A. Schaefer, O. Ambacher, F. M. Morales, J. G. Lozano, and D. González, J. Appl. Phys. **100**, 094902 (2006).

¹²V. Cimalla, J. Pezoldt, G. Ecke, R. Kosiba, O. Ambacher, L. Spieß, H. Lu, W. J. Schaff, and G. Teichert, Appl. Phys. Lett. **83**, 3468 (2003).

¹³Jae-Hong Lim, Dae-Kue Hwang, Hyun-Sik Kim, Jin-Yong Oh, Jin-Ho Yang, R. Navamathavan, and Seong-Ju Park, Appl. Phys. Lett. **85**, 6191 (2004).

¹⁴Ch. Y. Wang, V. Cimalla, H. Romanus, Th. Kups, G. Ecke, Th. Stauden, M. Ali, V. Lebedev, J. Pezoldt, and O. Ambacher, Appl. Phys. Lett. **89**, 011904 (2006).

¹⁵N. Nadaud, N. Lequeux, M. Nanot, J. Jove, and T. Roisnel, J. Solid State Chem. **135**, 140 (1998).

¹⁶X. J. Ning, F. R. Chien, P. Pirouz, J. W. Yang, and M. A. Khan, J. Mater. Res. **11**, 580 (1996).

¹⁷L. Mancera, J. A. Rodríguez, and N. Takeuchi, Phys. Status Solidi B **241**, 2424 (2004).

¹⁸A. Zoroddu, F. Bernardini, V. Fiorentini, and P. Ruggerone, Phys. Rev. B **64**, 045208 (2001).

¹⁹A. F. Wright, J. Appl. Phys. **82**, 5259 (1997).